

Error-Aware Imitation Learning from Teleoperation Data for Mobile Manipulation

Josiah Wong, Albert Tung, Andrey Kurenkov, Ajay Mandlekar,
Li Fei-Fei, Silvio Savarese, Roberto Martín-Martín

Stanford University

Abstract: In mobile manipulation (MM), robots can both navigate within and interact with their environment and are thus able to complete many more tasks than robots only capable of navigation or manipulation. In this work, we explore how to apply imitation learning (IL) to learn continuous visuo-motor policies for MM tasks. Much prior work has shown that IL can train visuo-motor policies for either manipulation or navigation domains, but few works have applied IL to the MM domain. Doing this is challenging for two reasons: on the data side, current interfaces make collecting high-quality human demonstrations difficult, and on the learning side, policies trained on limited data can suffer from covariate shift when deployed. To address these problems, we first propose MOBILE MANIPULATION ROBOTURK (MOMART), a novel teleoperation framework allowing simultaneous navigation and manipulation of mobile manipulators, and collect a first-of-its-kind large scale dataset in a realistic simulated kitchen setting. We then propose a learned error detection system to address covariate shift by detecting when an agent is in a potential failure state. We train performant IL policies and error detectors from this data, and achieve over 45% task success rate and 85% error detection success rate across multiple multi-stage tasks when trained on expert data. Codebase, datasets, visualization, and more available at <https://sites.google.com/view/il-for-mm/home>.

Keywords: Mobile Manipulation, Imitation Learning, Error Detection

1 Introduction

In mobile manipulation (MM), robots combine interaction and locomotion capabilities to substantially extend the depth and breadth of tasks they can perform compared to static manipulation [1, 2, 3, 4]. For example, in household environments MM agents can perform tasks such as cleaning up the dining table and bringing the dishes to the dishwasher. Data-driven paradigms such as reinforcement learning are attractive for MM since they enable such agents to learn directly from raw sensory observations, so that they can function in a wide variety of households. However, due to the many possible interactions that are possible for the agent (looking, navigating, and manipulating various parts of the household) the state space for MM tasks is vast, which imposes a difficult exploration burden for agents that learn autonomously. Learning from human demonstrations has been extremely effective in addressing the burden of exploration in static manipulation settings. Can we apply the same paradigm for mobile manipulation?

Unfortunately, the vast state space in MM has inhibited data collection from humans due to the difficulty of annotating substantial portions of the state space with good actions. Prior work has avoided this issue by instrumenting the environment to ease the state coverage burden [5, 6, 7, 8]. However, even if there were a way to collect full human demonstrations without instrumentation, learning from such datasets would also pose a challenge due to covariate shift [9], where trained policies visit states not covered by the demonstrations – an outcome that is more likely in MM. In this paper, we address the problem of collecting and learning from human demonstrations in mobile manipulation settings via two key solutions: a novel system to collect MM demonstrations, and an algorithmic framework that can detect when an agent is suffering from covariate shift.

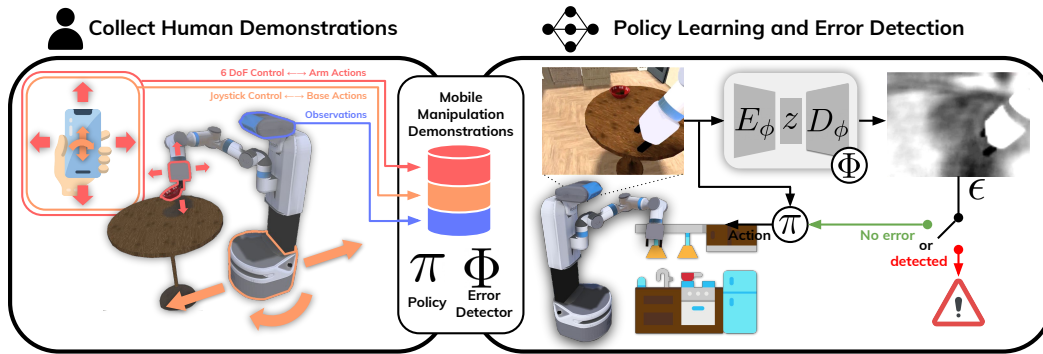


Figure 1: **Leveraging Human Demonstrations for Mobile Manipulation.** Humans have strong intuitions about how to move and interact based on visual data. We leverage their knowledge by first collecting human demonstrations teleoperating a mobile manipulator using MOMART (*left*), and proceed to train imitation learning policies and error detectors from the resulting dataset (*middle*). During rollouts, the policy executes actions continuously while the error detector simultaneously checks if the current visual state can be reconstructed. A sufficiently irregular state provokes the error detector to intervene, either resetting the agent to well-known configuration or immediately terminating to prevent erratic policy behavior (*right*).

First, we present MOBILE MANIPULATION ROBOTURK (MOMART), a novel teleoperation system that allows humans to remotely control mobile manipulators in a natural and easy manner. Operators control the robot’s motion using their smartphone to provide real-time navigation and manipulation commands simultaneously. Unlike prior works on IL for MM which leverage privileged information during demonstration collection, our system constrains the user to observing what the robot sees from its onboard cameras, resulting in more realistic trajectories and demonstrations that require minimal assumptions about the task at hand.

Second, recognizing that human data will be insufficient to cover all relevant states, we propose a new IL method that augments a trained policy with a learned error detector that can distinguish between in- and out-of-distribution states. When an agent encounters states previously unseen during training, our error detector can detect fatal errors and immediately stop the execution. In this way, our error detector can constrain the policy to execute only during states similar to what it has seen before, and prevent potentially unstable behavior from occurring during previously unseen states.

We demonstrate the potential of MOMART for mobile manipulation by generating the most general and largest dataset of mobile manipulation demonstrations publicly available: over 1200 demonstrations on five long-horizon tasks spanning expert, suboptimal, and few-shot generalization trajectories, totalling over 11 hours of simulation data. We use the dataset to train imitation learning policies that can achieve success rates greater than 45% and out-of-distribution detectors that achieve over 85% error detection success rate across all tasks.

In summary, our core contributions are as follows:

- We present MOMART, a novel teleoperation system that enables intuitive and expressive teleoperation of mobile manipulation robots,
- We collect a first-of-its kind continuous control dataset in a realistic simulated kitchen domain consisting of over 1200 successful demonstrations across five long-horizon tasks with multi-sensor modalities and ablation subsets with domain randomization,
- We train performant IL task policies that reach over 45% success across all tasks, and augment these policies with a learned error detector model that can accurately detect when the agent is in a failure state and immediately terminate, achieving over 85% precision and recall.

2 Related Work

Robotic Teleoperation for Mobile Manipulation: IL leverages human demonstrations to learn tasks such as stationary manipulation [10, 11, 12, 13] and navigation [14, 15, 16, 17]. Having human operators remotely control an agent, or teleoperation, is a common approach for collecting demonstrations. Teleoperation for MM is not easy to implement, as it requires enabling the user to control both navigation and manipulation, possibly simultaneously. Previous work on this

problem has explored using online click-through interfaces [18, 19, 20], muscle signals [21, 22], joysticks [23, 24, 25], tablets [26], and virtual reality interfaces [27, 28, 29, 30, 31, 32, 33, 34]. These approaches are either scalable or easy to use: web-based tools are widely available but are not well suited to demonstrate dexterous continuous control, while VR and other interfaces are intuitive to use but are not widely available. The new system we propose (Sec. 3) is both easy to use and scalable: the interface only requires a web browser for viewing and a phone that combines joystick and motion tracking capabilities for remote control of the agent [35].

Autonomous Mobile Manipulation: Algorithms for autonomous MM have been studied for decades [36, 37], and have primarily been addressed with either control [38, 39, 40, 41] or Task and motion planning (TaMP) [3, 42, 43, 44] approaches. Both are able to generalize across different robots, environments, and robots, but control approaches are generally limited to short horizon tasks, and TaMP approaches depend on human specification of the symbolic actions and full information about the 3D structure of the environment. To address these limitations, learning-based approaches have recently been applied to MM to learn a direct mapping from raw sensory observations to actions [45, 46, 47]. Due to the lack of explicit planning, these works suffer in long horizon tasks involving heterogeneous types of actions such as grasping and moving objects.

Most related to our work, several works have leveraged IL for MM tasks [5, 6, 7, 8]. [5] presented a web-based tool for crowdsourcing a large scale dataset of MM tasks, and used it in combination with motion planning for execution on the robot. [6] and [7] collected RGBD observations of humans performing tasks such as door opening and tabletop object manipulation, and used hypergraph optimization and a search procedure respectively to adapt these trajectories to be executable by a robot. Lastly, [8] collected VR demonstrations of pick and place actions and extracted a sequence of symbolic actions and action parametrizations to adopt them for use on a robot. While these works demonstrate using IL for complex MM tasks, their approaches are limited to using the demonstrations to parametrize execution of action primitives, and so do not apply to the problem of learning a general visuo-motor policy of arbitrary manipulation actions as we do in this paper.

Error Detection: A common approach to prevent robotic agents from reaching states that harm the environment or themselves is to detect out-of-distribution (OOD) inputs to the agent [48]. Most relevant to our work, various approaches have been proposed for detecting OOD states using deep neural network-based architectures, such as direct training of an error prediction mode [49], uncertainty estimation for the policy [50, 50, 51, 52], or computing a reconstruction error for the input [53, 54, 55, 56]. In this work we follow the latter approach by training a conditional autoencoder to predict a future goal state given a current state and using its reconstruction error to determine if the robot is in a bad state. While prior works have similarly utilized such errors for collision avoidance, we go beyond them with a multi-modal prior that captures better the multiple solutions that humans demonstrated to the same goal, and apply the concept for the first time in a MM setup.

3 Mobile Manipulation RoboTurk (MOMART)

In this section, we present our approach for collecting demonstrations for MM. We first discuss RoboTurk [35], the precursor to our system, and then present our novel MOMART teleoperation system enabling remote and intuitive control of mobile manipulators.

RoboTurk Overview: RoboTurk [35, 57] is a platform that enables remote teleoperation of real or simulated robot arms. An operator connects to a server, receives live video stream with observations from the robot camera on their web-browser, and controls the robot’s end-effector by moving a smartphone. The motion of the phone in Cartesian space (6 DoF, position and orientation) is tracked and mapped directly to the robot’s end-effector motion, and leverages Web Real-Time Communication (WebRTC) to enable real-time control. RoboTurk has been used to collect large datasets on simulated [35] and real arms [57], accelerating IL for robot manipulation research [58, 59]. However, the platform has been limited to stationary arm manipulation.

3.1 MOMART

Due to the limitations of the original RoboTurk platform, we design MOMART, an extension of the original RoboTurk platform that enables intuitive control all the degrees of freedom of a mobile manipulator. In MOMART, we assume that the mobile manipulator consists of a single arm, a non-

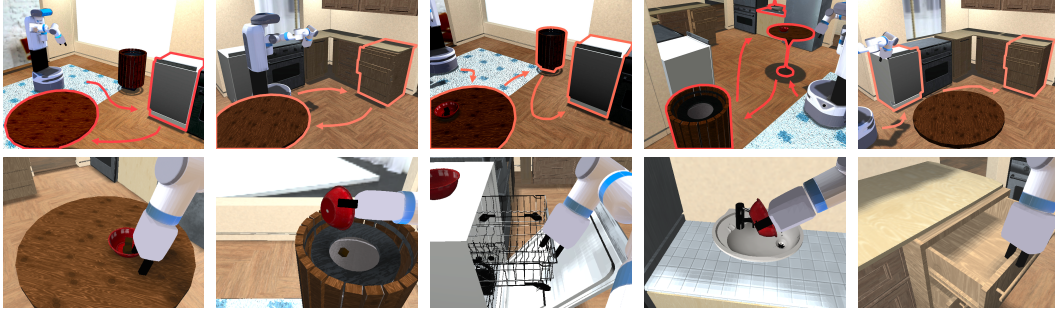


Figure 2: **Simulated Kitchen Tasks.** We present 5 challenging long-horizon mobile manipulation tasks requiring varied interactions with multiple household objects. *Top:* Tasks from left to right: Set Table from Dishwasher, Set Table from Dresser, Table Cleanup to Dishwasher, Table Cleanup to Sink, Unload Dishwasher to Dresser. *Bottom:* Our tasks evaluate an agent’s ability to execute diverse sets of manipulation and navigation skills, including accurate arm positioning and contact-rich, arm-base coordinated interaction of large constrained mechanisms. Teleoperators are limited to this ego-centric view, highlighting partial observability.

holonomic base, and a controllable head, such as the Fetch or PAL Tiago robots. We model our system close to real-robot hardware and plan to extend it to the real-world post-pandemic (Sec. A.10).

As evidenced by prior MM teleoperation platforms, designing a well-balanced interface can be challenging for multiple reasons: fully exploring MM requires simultaneous control of base and arm motion, but allowing control of all possible degrees of freedom can overload the operator and degrade the quality of the resulting demonstrations. Moreover, unlike static manipulation with a global fixed frame of reference, mobile manipulators often only have access to a local frame of reference, modified only by controlling the head. Finally, the long-horizon nature of MM increases the likelihood of demonstrations diverging over time, resulting in sparsely distributed end states.

We showcase our smartphone interface design in Fig. A.1 with all of these challenges in mind. Our platform is easy to use, enabling simultaneous 6DOF arm end-effector control through smartphone motion and base locomotion control through the on-screen joystick. To address the head control problem, we fix the head pan (horizontal) joint and allow the tilt (vertical) joint to automatically maintain the end-effector in the central area of the head camera frame. Lastly, recognizing that teleoperated robots can fall into bad configurations, we include a button-triggered arm-reset that generates a trajectory to move the arm to a pre-defined stable initial joint configuration. The reset helps regularize the arm state distribution observed during teleoperation and increases the consistency between demonstrations, and is leveraged in our final IL learning system with error detection to try and recover from mistakes (Sec. 4.3). Altogether, MOMART enables collecting of teleoperated demonstrations from remote locations with an intuitive interface that allows to simultaneous navigation and manipulation in complex environments. Further details can be found in Appendix A.4, and we also conduct a user study to qualitatively evaluate our system in Appendix A.5.

3.2 Simulated Kitchen Dataset

To evaluate the teleoperation capabilities of MOMART for MM and generate data for our novel IL with error detection algorithm (Sec. 4), we create five realistic multi-stage simulated household kitchen tasks and collect a large-scale multi-user demonstration dataset. We design the simulated tasks in a realistic kitchen environment using PyBullet [60] and the iGibson [61, 62] framework with a Fetch [63] robot that must manipulate a bowl. Across all tasks, the robot’s initial pose and bowl location is randomized between episodes. An overview of our tasks can be seen in Fig. 2 and are summarized in the following:

Table Cleanup to Dishwasher / Sink: The robot must navigate to the table, pick up the bowl with trash in it, navigate to the trashcan, and empty the trash. Then, it must either (a) take the bowl to the dishwasher, open the dishwasher and pull out the tray, and place the bowl into the tray, or (b) take the bowl to the sink and drop it in the basin. In addition to the robot and bowl, the trash can’s pose is also randomized between episodes. These tasks evaluate an agent’s ability to execute a diverse range of manipulation and navigation skills, including accurate arm positioning and contact-rich, arm-base coordinated interaction of large constrained mechanisms.

Table Setup from Dresser / Dishwasher: The robot must first either (a) navigate to the dresser, and search for the bowl by opening each drawer, or (b) navigate to and open the dishwasher, and then pull out the tray. Afterwards, in both cases, it must grab the bowl, and navigate to the table and drop off the bowl. In addition to local randomization, the bowl’s location is also randomized across the drawers between episodes. Searching the dresser evaluates an agent’s ability to contextualize its observations on prior actions.

Unload Dishwasher to Dresser: The robot must first navigate to the dishwasher and grab the bowl. Then, it must navigate to the dresser, open the top drawer, and place the bowl inside. This task evaluates an agent’s ability to avoid obstacles based on estimated visual states.

For each task, we use MOMART to collect over 110 successful demonstrations per task from both an expert and suboptimal operator, as well as additional few-shot generalization subsets consisting of over 20 demonstrations where key task furniture items have changed significantly their locations, producing a dataset that includes over **1200 successful demonstrations** totalling **over 11 hours of data**. This is a first of its kind large-scale human demonstration dataset of continuous control collected on realistic long-horizon tasks in the MM setting, and we hope this dataset facilitates future research in IL for MM.

4 Learning Mobile Manipulation from Human Demonstrations

In this section, we present our approach for IL for MM. After some preliminaries, we introduce our modified temporal network architecture with more efficient temporal abstraction for IL of MM, and then propose an error detection model that can distinguish between in- and out-of-distribution states to alleviate the challenges of the unbounded state space in MM.

4.1 Preliminaries

Partial Observability. We formalize the problem of solving a robot MM task as an infinite-horizon discrete-time Partially Observable Markov Decision Process (POMDP). At every step, an agent in state s_t receives an observation o_t and uses a policy π to choose an action, $a_t = \pi(o_t, o_{t-1}, \dots)$, which moves it to state s_{t+1} according to the state transition distribution.

Imitation Learning: We train a visuo-motor continuous control policy for MM with a variant of Behavioral Cloning (BC) [64]. The policy maps observations to base and arm actions for the mobile manipulator. BC trains a policy, $\pi_\theta(o)$, from a set of demonstrations, \mathcal{D} , by minimizing the objective: $\arg \min_\theta \mathbb{E}_{(o,a) \sim \mathcal{D}} \|\pi_\theta(o) - a\|^2$. We base our policy on a variant of BC that leverages temporal abstraction, BC-RNN, in which the policy is parameterized by a recurrent neural network (RNN) that is trained on T -length temporal observation-action sequences to produce an action sequence, a_t, \dots, a_{t+T-1} . To account for the possibility of multi-modal possibilities in a given state, actions are parameterized by a Gaussian Mixture Model (GMM) distribution [65], $a_t \sim \sum_i^N w_i \mathcal{N}(\mu_i, \sigma_i)$, where actions are sampled from amongst N weighted individual Gaussian distributions.

4.2 TieredRNN

Prior work on learning from human demonstrations in robotic manipulation domains has shown substantial benefits from models leveraging temporal abstraction [58, 66]. Inspired by these works, we extend the RNN model from BC-RNN into a multi-layered variant (TieredRNN). This new variant integrates multiple layers operating at varying timesteps to better streamline information flow from timesteps early on in a given sequence to timesteps much further downstream, which can be useful for our long-horizon MM tasks.

The TieredRNN consists of N individual RNN layers (“tiers”), with corresponding timestep periods τ_1, \dots, τ_N , $\tau_1 < \dots < \tau_N$. For given sequence of length T , $t = t, t+1, \dots, t+T$ and corresponding states $s_t, s_{t+1}, \dots, s_{t+T}$, layer i updates its hidden state if $\tau_i \bmod t = 0$ and outputs a M -dim encoding vector z_i , which gets passed in addition to s_t to the immediate preceding $i-1$ layer. The output of the final layer $i=1$ is the overall output of the TieredRNN. In this way, information at varying levels of temporal abstraction can be preserved across many timesteps and better inform an agent of past context. We refer to BC agents using this temporal structure as BC-TieredRNN agents.

Task	ReLMoGen ¹	BC-RNN Suboptimal	BC-TieredRNN Suboptimal	BC-RNN Expert	BC-TieredRNN Expert
Table Cleanup to Dishwasher	0.0 ± 0.0	16.0 ± 5.5	20.8 ± 5.0	44.4 ± 4.0	47.8 ± 7.3
Table Cleanup to Sink	0.0 ± 0.0	10.4 ± 5.2	8.9 ± 2.9	54.4 ± 7.1	61.1 ± 3.1
Table Setup from Dresser	0.0 ± 0.0	20.0 ± 0.9	17.8 ± 4.8	64.8 ± 5.8	68.1 ± 3.4
Table Setup from Dishwasher	0.0 ± 0.0	63.7 ± 7.7	61.1 ± 3.1	68.5 ± 7.6	66.2 ± 2.3
Unload Dishwasher to Dresser	0.0 ± 0.0	11.9 ± 4.5	31.1 ± 7.4	56.0 ± 7.0	47.8 ± 8.1

¹We include more extensive results in Appendix A.6

Table 1: **Simulated Kitchen Tasks Results:** IL can solve all of our multi-stage tasks, whereas RL (ReLMoGen) cannot solve any task and in all tasks is unable to even grasp the bowl as is detailed in Appendix A.6. When trained on expert data, our BC-TieredRNN model can achieve over 45% success rate over all tasks, and outperforms all other baselines on a majority of the tasks.

4.3 Error Detection and Intervention Functionality

One of the central challenges of IL for MM is the unbounded state space that the robot can explore, since states that sufficiently differ from collected human demonstrations can cause an IL policy to quickly degrade. This common covariate shift problem [9] of IL is thus exacerbated by the MM setup. While it is difficult to alleviate this problem without collecting additional online samples, we propose a simple but effective method for detecting errors and improving the overall safety of policy execution by leveraging our demonstration data as a strong prior for distinguishing between in- and out-of-distribution states (Fig. 1).

Detecting Errors. Similar to prior work, our error detector Φ leverages a variational autoencoder (VAE) [67] and its reconstruction error ϵ as a proxy for distinguishing in- and out-of-distribution states. In our setting, this means that with sufficient training data and capacity, Φ should learn to reconstruct similar states to those observed from the demonstrations with low ϵ . We leverage ϵ for distinguishing between in- and out-of-distribution states: abnormally high ϵ likely correspond to unseen states and can be interpreted as failure modes during rollouts. Implementation details can be found in Appendix A.2.

Intervening During Errors. We implement two discrete intervention actions that can be triggered when an error is detected. `recover` is triggered the first time an error is encountered, and moves the agent to a default pose to allow it to re-attempt execution. If the `recover` action fails to bring the error level below the threshold, or if K errors have been detected within a given rollout, the error detector executes `terminate`, which immediately terminates the episode. In this way, even if an error is unrecoverable, the agent can detect and respond to its circumstance (for example, asking a human for help). Crucially, because our error detector and policy are not provided any additional online data, we do not expect the `recover` action to consistently succeed. However, we do expect our `terminate` intervention to be consistent and reliable as it relies solely on our error detector’s ability to consistently detect out-of-distribution states; this is essential for mitigating potentially harmful policy behavior resulting from covariate shift. Algorithm 1 formalizes our method.

5 Experimental Evaluation

In this section, we first evaluate our IL algorithm for MM, BC-TieredRNN, and compare to baselines of IL and RL, BC-RNN, and ReLMoGen [45]. ReLMoGen is a state-of-the-art RL-based algorithm that leverages discrete actions with a motion planner. Then, we train and evaluate our error detector and recovery for MM, and show that it can accurately detect out-of-distribution states and either help the agent recover to in-distribution states or know when to terminate due to unrecoverable errors. Videos and other results can be seen at <https://sites.google.com/view/il-for-mm/home>. Specific training and hyperparameter details can be found in Appendix, Sec. A.1 and A.3.

5.1 Simulated Results: Solving Long-Horizon Mobile Manipulation Tasks

For each task, we train each model for 30 epochs and record the average top three best evaluation success rates from 30 episodes aggregated over 3 seeds. For ReLMoGen, we use a shaped reward for each task and train the agent for 200K time steps. Our results can be seen in Table 1.

Imitation Learning Outperforms Reinforcement Learning. We observe that ReLMoGen cannot solve any task despite its lifted action space and shaped reward. This highlights the exploration burden exacerbated in the MM setup, which can cause current state-of-the-art RL methods to completely flatline. In contrast, our IL methods can perform well and achieve success learning end-to-end visuo-motor policies on these multi-stage MM tasks.

On the expert dataset, we find that our BC-TieredRNN model outperforms the BC-RNN baseline in the tasks where memory is critical: *Table Cleanup to Dishwasher* and *Table Cleanup to Sink*, both of which have randomized locations of the trash bin, and *Table Setup from Dresser*, where the bowl can be located in multiple drawers. In these tasks where the agent must remember where it has been in the past, we hypothesize that the TieredRNN is better equipped to allow long-term information flow through its skip-connection architecture. In contrast, in the tasks that do not require randomization (*Table Setup from Dishwasher* and *Unload Dishwasher to Dresser*), the TieredRNN provides no benefit and is instead outperformed by BC-RNN. We further contextualize our usage of the TieredRNN model in Appendix A.7.

Demonstration Quality Dictates Success. With the exception of *Table Setup from Dishwasher*, we observe on average over 200% increase in success rate when training on the same number of expert demonstrations compared to suboptimal demonstrations. In the latter case, the operators were new to using the MOMART system, whereas the expert operator had prior experience. This both showcases the ability of our platform to produce impressive results on multiple long-horizon MM tasks given experience, and also highlights the importance of the teleoperation interface for collecting high-quality demonstrations that better facilitate learning.

5.2 Simulated Results: Detecting Errors During Rollout

For each task, we train our error detector and set a uniform error threshold $\psi = 0.05$ based on analysis from a small number of expert rollouts. Because the BC-TieredRNN model performed the best on the majority of tasks, we utilize this model for error detection evaluation. We evaluate our error detector’s performance when paired with the trained policy model, and record the precision ($\frac{n_{\text{post}}}{n_{\text{post}} + n_{\text{pos}_f}}$) and recall ($\frac{n_{\text{post}}}{n_{\text{post}} + n_{\text{neg}_f}}$). Because we are in simulation, we can deterministically evaluate the counterfactual between the model augmented with the error detector and the same model without. A true / false positive occurs when the error detector detects an error when the original model fails / succeeds, respectively. Likewise, a true / false negative occurs when the error detector does not trigger during a successful / failed rollout, respectively. Metrics are aggregated over the 3 policy seeds each evaluated on 30 rollouts with mean and standard deviations shown in Table 2.

Errors are Reliably and Robustly Detected. We find that our error detectors can consistently detect errors and achieve over 85% precision and recall rates across all tasks when trained on the expert dataset. The high precision means that our error detectors can accurately distinguish between error and non-error states, and the high recall means that it can also reliably detect true errors when they occur. This is especially important in MM domains where learned agents can easily diverge into unseen states during rollouts and become erratic if left unchecked.

While the error detectors occasionally misfire, and causes a marginal decrease in success, we observe that the success rates remains generally consistent. This highlights that our error detector is not overly conservative and does not prematurely terminate episodes when there is no true error at hand. Interestingly, in some cases, such as in *Table Setup from Dresser*, the `recover` action of our error detector is able to result in marginal policy improvement. While unexpected, this suggests that similar methods bringing a robot back into well-known states may provide benefits for MM agents.

Data Diversity Impacts Error Detection When trained on suboptimal data, our error detectors surprisingly achieve over 90% precision across all tasks. However, the recall rate substantially suffers. We postulate that this is due to the noisy nature of the suboptimal data encompassing a wider distribution of states, augmenting the resulting error detectors’ abilities to reject non-error states while making it more difficult to consistently detect true error states.

Our Error Detector is Interpretable and Easily Tuned. While we deployed all error detectors with the same uniform error threshold value ϵ , each error detector can be individually tuned in an interpretable way. For example, lowering ϵ increases the error detector’s sensitivity to observation irregularities, thereby improving the likelihood of detecting true errors (increased recall), at the potential cost of additional spurious error triggers (decreased precision). This can be useful in

Dataset	Task	SR (no ED)	SR (ED)	ED Precision	ED Recall
Expert	Table Cleanup to Dishwasher	34.4 ± 10.3	32.2 ± 8.7	96.4 ± 2.6	100.0 ± 0.0
	Table Cleanup to Sink	51.1 ± 4.2	51.1 ± 4.2	97.2 ± 3.9	86.5 ± 10.3
	Table Setup from Dresser	63.3 ± 7.2	65.6 ± 8.7	100.0 ± 0.0	85.9 ± 10.0
	Table Setup from Dishwasher	51.1 ± 6.8	47.8 ± 11.0	88.2 ± 10.2	100.0 ± 0.0
	Unload Dishwasher to Dresser	36.7 ± 10.9	33.3 ± 9.8	85.8 ± 5.3	100.0 ± 0.0
Suboptimal	Table Cleanup to Dishwasher	16.7 ± 4.7	22.2 ± 8.3	93.4 ± 5.3	76.9 ± 18.8
	Table Cleanup to Sink	1.1 ± 1.5	1.1 ± 1.5	98.4 ± 2.2	66.3 ± 7.1
	Table Setup from Dresser	7.7 ± 6.3	15.6 ± 4.2	97.6 ± 3.4	58.7 ± 7.4
	Table Setup from Dishwasher	52.2 ± 4.2	48.9 ± 5.7	90.0 ± 7.7	95.2 ± 6.7
	Unload Dishwasher to Dresser	26.7 ± 2.7	26.7 ± 2.7	94.6 ± 3.9	44.2 ± 14.1
Few-Shot Generalize	Table Cleanup to Dishwasher	13.3 ± 4.7	6.7 ± 2.7	91.2 ± 4.9	94.8 ± 3.7
	Table Cleanup to Sink	24.4 ± 6.8	11.1 ± 6.8	80.6 ± 3.7	98.7 ± 1.9
	Table Setup from Dresser	8.8 ± 8.3	7.8 ± 8.7	98.0 ± 2.8	64.4 ± 6.7
	Table Setup from Dishwasher	40.0 ± 16.3	24.4 ± 12.9	78.2 ± 10.6	100.0 ± 0.0
	Unload Dishwasher to Dresser	2.2 ± 1.6	2.2 ± 1.6	98.9 ± 1.6	100.0 ± 0.0

Table 2: **Error Detection Results** When trained on expert data, our error detectors can accurately detect errors, achieving over 85% precision and recall across all tasks. With suboptimal data, the error detectors can similarly reject non-error states consistently but can struggle to detect true error states. Lastly, the error detectors can adapt to the few-shot generalization setting, maintaining high precision and recall despite the generalized policy’s significant deterioration.

situations where safety is critical and the additional confidence in reliable error detection is worth the cost of lowered success rate. Further results comparing our method against potential alternatives can be seen in Appendix A.8.

5.3 Simulated Results: Few-Shot Generalization

Lastly, we evaluate the generalizability of our policy and error detector by taking the models trained on the expert data and finetuning them on the few-shot demonstrations exhibiting major distribution shift, where the critical furniture objects (dishwasher, dresser, and sink) have swapped places. Similar to Sec.5.2, we evaluate the success with and without the error detector, and also report the corresponding detection metrics, shown at the bottom of Table 2.

Imitation Learning Has Potential to Generalize With Little Additional Data. While the success rates drop significantly compared to the original baselines, we find that our model can still solve the task given only a limited number of successful demonstrations in this generalized setting. These results show promise for IL to lower the data burden for learning general visuomotor policies in similar MM settings as our kitchen environment, where the discrete number of unique object instances is finite but the combinatorial possibilities are huge. Appendix A.9 highlights the benefits of finetuning versus training solely on the few-shot demonstrations.

Error Detection Can Adapt to Distribution Shifts. Even in this generalized setting, our error detector still performs well, and often achieves more than 80% precision and 90% recall across all tasks. This shows how our detector, once initially trained, can quickly adapt its modeled state distribution to account for new training data and still accurately detect true error states while ignoring non-error states.

6 Conclusion

We presented three contributions for IL in MM setups. First, we introduced MOMART, a novel teleoperation platform for MM. Second, we used MOMART collect a first of its kind large-scale MM dataset of continuous control. And third, we presented variants of IL and error detection for the MM setup that train performant visuo-motor policies and accurately detect errors. Our next step after the pandemic is to bring our new teleoperation interface to control a real mobile manipulator (Sec. A.10). We hope our diverse dataset can provide researchers the accessible means to investigate many other important problems in MM from an IL perspective.

Acknowledgments

We would like to thank Jiangshan Li for her help in setting up the initial RoboTurk prototype.

References

- [1] B. Siciliano and O. Khatib. *Springer handbook of robotics*. springer, 2016.
- [2] O. Khatib. Mobile manipulation: The robotic assistant. *Robotics and Autonomous Systems*, 26(2-3):175–183, 1999.
- [3] J. Wolfe, B. Marthi, and S. Russell. Combined task and motion planning for mobile manipulation. In *Twentieth International Conference on Automated Planning and Scheduling*, 2010.
- [4] S. Tellex, T. Kollar, S. Dickerson, M. Walter, A. Banerjee, S. Teller, and N. Roy. Understanding natural language commands for robotic navigation and mobile manipulation. In *Proceedings of the AAAI Conference on Artificial Intelligence*, volume 25, 2011.
- [5] E. Ratner, B. Cohen, M. Phillips, and M. Likhachev. A web-based infrastructure for recording user demonstrations of mobile manipulation tasks. In *2015 IEEE International Conference on Robotics and Automation (ICRA)*, pages 5523–5530, 2015. doi:10.1109/ICRA.2015.7139971.
- [6] T. Welschhold, C. Dornhege, and W. Burgard. Learning mobile manipulation actions from human demonstrations. In *2017 IEEE/RSJ International Conference on Intelligent Robots and Systems (IROS)*, pages 3196–3201. IEEE, 2017.
- [7] T. Welschhold, N. Abdo, C. Dornhege, and W. Burgard. Combined task and action learning from human demonstrations for mobile manipulation applications. In *2019 IEEE/RSJ International Conference on Intelligent Robots and Systems (IROS)*, pages 4317–4324. IEEE, 2019.
- [8] G. Kazhoyan, A. Hawkin, S. Koralewski, A. Haidu, and M. Beetz. Learning motion parameterizations of mobile pick and place actions from observing humans in virtual environments. In *2020 IEEE/RSJ International Conference on Intelligent Robots and Systems (IROS)*, pages 9736–9743. IEEE, 2020.
- [9] S. Ross, G. Gordon, and D. Bagnell. A reduction of imitation learning and structured prediction to no-regret online learning. In *Proceedings of the fourteenth international conference on artificial intelligence and statistics*, pages 627–635. JMLR Workshop and Conference Proceedings, 2011.
- [10] S. Schaal. Is imitation learning the route to humanoid robots? *Trends in Cognitive Sciences*, 3:233–242, 1999.
- [11] A. Billard, S. Calinon, R. Dillmann, and S. Schaal. Robot programming by demonstration. In *Springer Handbook of Robotics*, 2008.
- [12] S. Calinon, F. D’halluin, E. L. Sauser, D. G. Caldwell, and A. Billard. Learning and reproduction of gestures by imitation. *IEEE Robotics and Automation Magazine*, 17:44–54, 2010.
- [13] B. D. Argall, S. Chernova, M. Veloso, and B. Browning. A survey of robot learning from demonstration. *Robotics and autonomous systems*, 57(5):469–483, 2009.
- [14] A. Hussein, E. Elyan, M. M. Gaber, and C. Jayne. Deep imitation learning for 3d navigation tasks. *Neural computing and applications*, 29(7):389–404, 2018.
- [15] P. M. Kebria, A. Khosravi, I. Hossain, N. Mohajer, H. D. Kabir, S. M. J. Jalali, D. Nahavandi, S. M. Salaken, S. Nahavandi, A. Lagrandcourt, et al. Autonomous navigation via deep imitation and transfer learning: A comparative study. In *2020 IEEE International Conference on Systems, Man, and Cybernetics (SMC)*, pages 2907–2912. IEEE, 2020.
- [16] J. Xu, Q. Liu, H. Guo, A. Kageza, S. AlQarni, and S. Wu. Shared multi-task imitation learning for indoor self-navigation. In *2018 IEEE Global Communications Conference (GLOBECOM)*, pages 1–7. IEEE, 2018.

- [17] H. Karnan, G. Warnell, X. Xiao, and P. Stone. Voila: Visual-observation-only imitation learning for autonomous navigation. *arXiv preprint arXiv:2105.09371*, 2021.
- [18] D. Wang, J. Yi, D. Zhao, and G. Yang. Teleoperation system of the internet-based omnidirectional mobile robot with a mounted manipulator. In *2007 International Conference on Mechatronics and Automation*, pages 1799–1804. IEEE, 2007.
- [19] V. Annem, P. Rajendran, S. Thakar, and S. K. Gupta. Towards remote teleoperation of a semi-autonomous mobile manipulator system in machine tending tasks. In *International Manufacturing Science and Engineering Conference*, volume 58745, page V001T02A027. American Society of Mechanical Engineers, 2019.
- [20] J. Yan, J. Zhao, C. Yang, Y. Zhu, L. Ma, and Z. Chen. Design of a coordinated control strategy for multi-mobile-manipulator cooperative teleoperation system. In *2012 IEEE International Conference on Mechatronics and Automation*, pages 783–788. IEEE, 2012.
- [21] B. Wang, Z. Li, W. Ye, and Q. Xie. Development of human-machine interface for teleoperation of a mobile manipulator. *International Journal of Control, Automation and Systems*, 10(6): 1225–1231, 2012.
- [22] M. Zucker, S. Joo, M. X. Grey, C. Rasmussen, E. Huang, M. Stilman, and A. Bobick. A general-purpose system for teleoperation of the drc-hubo humanoid robot. *Journal of Field Robotics*, 32(3):336–351, 2015.
- [23] D. Ryu, J.-B. Song, C. Cho, S. Kang, and M. Kim. Development of a six dof haptic master for teleoperation of a mobile manipulator. *Mechatronics*, 20(2):181–191, 2010.
- [24] M. Stilman, K. Nishiwaki, and S. Kagami. Humanoid teleoperation for whole body manipulation. In *2008 IEEE International Conference on Robotics and Automation*, pages 3175–3180. IEEE, 2008.
- [25] C.-H. King, T. L. Chen, Z. Fan, J. D. Glass, and C. C. Kemp. Dusty: an assistive mobile manipulator that retrieves dropped objects for people with motor impairments. *Disability and Rehabilitation: Assistive Technology*, 7(2):168–179, 2012.
- [26] D. A. Lopez, J. A. Frank, and V. Kapila. Comparing interface elements on a tablet for intuitive teleoperation of a mobile manipulator. In *ASME 2014 12th Biennial Conference on Engineering Systems Design and Analysis*. American Society of Mechanical Engineers Digital Collection, 2014.
- [27] A. U. Krishnan. *Nursing Robot Teleoperation via Motion Mapping Interfaces*. PhD thesis, WORCESTER POLYTECHNIC INSTITUTE, 2020.
- [28] C. Gan, J. Schwartz, S. Alter, M. Schrimpf, J. Traer, J. De Freitas, J. Kubilius, A. Bhandwadar, N. Haber, M. Sano, et al. Threedworld: A platform for interactive multi-modal physical simulation. *arXiv preprint arXiv:2007.04954*, 2020.
- [29] A. Garcia-Garcia, P. Martinez-Gonzalez, S. Oprea, J. A. Castro-Vargas, S. Orts-Escolano, J. Garcia-Rodriguez, and A. Jover-Alvarez. The robotrix: An extremely photorealistic and very-large-scale indoor dataset of sequences with robot trajectories and interactions. In *2018 IEEE/RSJ International Conference on Intelligent Robots and Systems (IROS)*, pages 6790–6797. IEEE, 2018.
- [30] P. Martinez-Gonzalez, S. Oprea, A. Garcia-Garcia, A. Jover-Alvarez, S. Orts-Escolano, and J. Garcia-Rodriguez. Unrealrox: An extremely photorealistic virtual reality environment for robotics simulations and synthetic data generation. *arXiv preprint arXiv:1810.06936*, 2018.
- [31] F. Stramandinoli. Robot learning from human demonstration in virtual reality. 03 2018.
- [32] X. Gao, R. Gong, T. Shu, X. Xie, S. Wang, and S.-C. Zhu. Vrkitcchen: an interactive 3d virtual environment for task-oriented learning. *arXiv preprint arXiv:1903.05757*, 2019.

- [33] J. DelPreto, J. I. Lipton, L. Sanneman, A. J. Fay, C. Fourie, C. Choi, and D. Rus. Helping robots learn: A human-robot master-apprentice model using demonstrations via virtual reality teleoperation. In *2020 IEEE International Conference on Robotics and Automation (ICRA)*, pages 10226–10233. IEEE, 2020.
- [34] T. Zhang, Z. McCarthy, O. Jow, D. Lee, K. Goldberg, and P. Abbeel. Deep imitation learning for complex manipulation tasks from virtual reality teleoperation. *arXiv preprint arXiv:1710.04615*, 2017.
- [35] A. Mandlekar, Y. Zhu, A. Garg, J. Booher, M. Spero, A. Tung, J. Gao, J. Emmons, A. Gupta, E. Orbay, et al. Roboturk: A crowdsourcing platform for robotic skill learning through imitation. In *Conference on Robot Learning*, pages 879–893. PMLR, 2018.
- [36] W. F. Carriker, P. K. Khosla, and B. H. Krogh. Path planning for mobile manipulators for multiple task execution. *IEEE Transactions on Robotics and Automation*, 7(3):403–408, 1991.
- [37] K. Nagatani and S. Yuta. Designing strategy and implementation of mobile manipulator control system for opening door. In *Proceedings of IEEE International Conference on Robotics and Automation*, volume 3, pages 2828–2834. IEEE, 1996.
- [38] M. V. Minniti, F. Farshidian, R. Grandia, and M. Hutter. Whole-body mpc for a dynamically stable mobile manipulator. *IEEE Robotics and Automation Letters*, 4(4):3687–3694, 2019.
- [39] J. Pankert and M. Hutter. Perceptive model predictive control for continuous mobile manipulation. *IEEE Robotics and Automation Letters*, 5(4):6177–6184, 2020.
- [40] D. Honerkamp, T. Welschehold, and A. Valada. Learning kinematic feasibility for mobile manipulation through deep reinforcement learning. *arXiv preprint arXiv:2101.05325*, 2021.
- [41] M. Mittal, D. Hoeller, F. Farshidian, M. Hutter, and A. Garg. Articulated object interaction in unknown scenes with whole-body mobile manipulation, 2021.
- [42] C. R. Garrett, T. Lozano-Perez, and L. P. Kaelbling. Ffrob: Leveraging symbolic planning for efficient task and motion planning. *The International Journal of Robotics Research*, 37(1): 104–136, 2018.
- [43] S. Cambon, F. Gravot, and R. Alami. A robot task planner that merges symbolic and geometric reasoning. In *ECAI*, volume 16, page 895, 2004.
- [44] M. Stilman, J.-U. Schamburek, J. Kuffner, and T. Asfour. Manipulation planning among movable obstacles. In *Proceedings 2007 IEEE international conference on robotics and automation*, pages 3327–3332. IEEE, 2007.
- [45] F. Xia, C. Li, R. Martín-Martín, O. Litany, A. Toshev, and S. Savarese. Relmogen: Leveraging motion generation in reinforcement learning for mobile manipulation, 2021.
- [46] C. Li, F. Xia, R. Martín-Martín, and S. Savarese. Hrl4in: Hierarchical reinforcement learning for interactive navigation with mobile manipulators. In *Conference on Robot Learning*, pages 603–616. PMLR, 2020.
- [47] C. Wang, Q. Zhang, Q. Tian, S. Li, X. Wang, D. Lane, Y. Petillot, and S. Wang. Learning mobile manipulation through deep reinforcement learning. *Sensors*, 20(3):939, 2020.
- [48] R. Chalapathy and S. Chawla. Deep learning for anomaly detection: A survey. *arXiv preprint arXiv:1901.03407*, 2019.
- [49] S. Hecker, D. Dai, and L. Van Gool. Failure prediction for autonomous driving. In *2018 IEEE Intelligent Vehicles Symposium (IV)*, pages 1792–1799. IEEE, 2018.
- [50] G. Kahn, A. Villafior, V. Pong, P. Abbeel, and S. Levine. Uncertainty-aware reinforcement learning for collision avoidance. *arXiv preprint arXiv:1702.01182*, 2017.
- [51] A. Filos, P. Tigas, R. McAllister, N. Rhinehart, S. Levine, and Y. Gal. Can autonomous vehicles identify, recover from, and adapt to distribution shifts? *arXiv preprint arXiv:2006.14911*, 2020.

- [52] K. Menda, K. Driggs-Campbell, and M. J. Kochenderfer. Ensembledagger: A bayesian approach to safe imitation learning. In *2019 IEEE/RSJ International Conference on Intelligent Robots and Systems (IROS)*, pages 5041–5048. IEEE, 2019.
- [53] D. A. Pomerleau. Input reconstruction reliability estimation. In *Neural Network Perception for Mobile Robot Guidance*, pages 133–150. Springer, 1993.
- [54] C. Richter and N. Roy. Safe visual navigation via deep learning and novelty detection. In *Robotics: Science and Systems*, 2017.
- [55] N. Hirose, A. Sadeghian, M. Vázquez, P. Goebel, and S. Savarese. Gonet: A semi-supervised deep learning approach for traversability estimation. In *2018 IEEE/RSJ International Conference on Intelligent Robots and Systems (IROS)*, pages 3044–3051. IEEE, 2018.
- [56] M. A. Lee, M. Tan, Y. Zhu, and J. Bohg. Detect, reject, correct: Crossmodal compensation of corrupted sensors. *arXiv preprint arXiv:2012.00201*, 2020.
- [57] A. Mandlekar, J. Booher, M. Spero, A. Tung, A. Gupta, Y. Zhu, A. Garg, S. Savarese, and L. Fei-Fei. Scaling robot supervision to hundreds of hours with roboturk: Robotic manipulation dataset through human reasoning and dexterity. *arXiv preprint arXiv:1911.04052*, 2019.
- [58] A. Mandlekar, D. Xu, R. Martín-Martín, S. Savarese, and L. Fei-Fei. Learning to generalize across long-horizon tasks from human demonstrations. *arXiv preprint arXiv:2003.06085*, 2020.
- [59] A. Tung, J. Wong, A. Mandlekar, R. Martín-Martín, Y. Zhu, L. Fei-Fei, S. Savarese, D. Xu, R. Martín-Martín, A. Kurenkov, et al. Learning multi-arm manipulation through collaborative teleoperation. In *IEEE International Conference on Robotics and Automation (ICRA)*, 2020.
- [60] E. Coumans and Y. Bai. Pybullet, a python module for physics simulation for games, robotics and machine learning. <http://pybullet.org>, 2016–2021.
- [61] F. Xia, W. B. Shen, C. Li, P. Kasimbeg, M. E. Tchapmi, A. Toshev, R. Martín-Martín, and S. Savarese. Interactive gibbon benchmark: A benchmark for interactive navigation in cluttered environments. *IEEE Robotics and Automation Letters*, 5(2):713–720, 2020.
- [62] B. Shen, F. Xia, C. Li, R. Martín-Martín, L. Fan, G. Wang, S. Buch, C. D’Arpino, S. Srivastava, L. P. Tchapmi, et al. igibson, a simulation environment for interactive tasks in large realistic scenes. *arXiv preprint arXiv:2012.02924*, 2020.
- [63] M. Wise, M. Ferguson, D. King, E. Diehr, and D. Dymesich. Fetch & freight : Standard platforms for service robot applications. 2016.
- [64] D. A. Pomerleau. Alvin: An autonomous land vehicle in a neural network. In *Advances in neural information processing systems*, pages 305–313, 1989.
- [65] D. Reynolds. *Gaussian Mixture Models*, pages 659–663. Springer US, Boston, MA, 2009. ISBN 978-0-387-73003-5. doi:10.1007/978-0-387-73003-5_196. URL https://doi.org/10.1007/978-0-387-73003-5_196.
- [66] A. Tung, J. Wong, A. Mandlekar, R. Martín-Martín, Y. Zhu, L. Fei-Fei, and S. Savarese. Learning multi-arm manipulation through collaborative teleoperation, 2020.
- [67] D. P. Kingma and M. Welling. Auto-encoding variational bayes. *arXiv preprint arXiv:1312.6114*, 2013.

Appendix A: Experiment Details

A.1 Task Setup

Here, we describe the inputs and outputs of our environment. Actions are executed at 20Hz and consist of a 10-dimensional command $[a_{base}, a_{arm}]$, where $a_{base} = [v_{lin}, v_{ang}] \in (-1, 1)^2$ is the differential drive velocity commands for the base; and $a_{arm} = [dx, dy, dz, da_x, da_y, da_z, grasp, reset] \in (-1, 1)^8$, where $[dx, dy, dz, da_x, da_y, da_z]$ is the 6DOF normalized delta commands in Cartesian space passed to an IK controller, $grasp > 0$ commands the gripper to close, and $reset > 0$ overrides the 6DOF delta command and instead moves the arm towards a pre-defined default pose. Observations consist of the head camera and wrist camera RGB-D frames (90 x 120), and the base laser scanner’s point cloud (1 x 100).

A.2 Error Detection Architecture

Our error detector $\Phi(s, s_g)$ consists of a conditional variational auto-encoder (cVAE): $E_\phi(s_g, s), D_\phi(z, s)$, where encoder E_ϕ maps the current state s , and the goal state s_g that is H steps into the future, into a gaussian mixture model (GMM) latent space distribution $z \sim \text{GMM}(\mu_1, \dots, \mu_n, \sigma_1, \dots, \sigma_n)$. The decoder D_ϕ then tries to reconstruct goal state s_g from the sampled latent embedding z conditioned on current state s_t .

There are two reasons why we choose this specific architecture. Reconstructing future goals conditioned on the current state enables our error detector to leverage temporal information to better inform its error prediction by implicitly coupling the likelihood of the future to the observations in the present. Secondly, using a GMM as the encoder’s prior can be useful in MM and other long-horizon settings where demonstrations can be diverse and result in more complex state distributions that need to be modeled.

The cVAE is trained using a weighted combination of KL Divergence loss to regularize the learned GMM distribution and reconstruction error ϵ to encourage salient encoded distributions. With sufficient training data and capacity, the cVAE Φ should learn to reconstruct similar states to those observed from the demonstrations with low ϵ . We leverage ϵ for distinguishing between in- and out-of-distribution states: abnormally high ϵ likely correspond to unseen states and can be interpreted as failure modes during rollouts.

While we have immediate access to all states at train time, we cannot directly apply this method during rollouts because we do not know a priori the future goal states s_g . Instead, we apply our error detector in the backwards direction: at timestep $t > H$, having recorded the prior H states in replay buffer β , we run the forward pass through our cVAE’s encoder E_ϕ and decoder D_ϕ with $s = s_{t-H}$ and $s_g = s_t$. In this way, the model peers retroactively into the past and considers the plausibility of the current state as a future goal from the perspective of the past.

A.3 Hyperparameters

In Table A.1, we present the hyperparameters used for training our policy and error detector, selected from a small-scale hyperparameter sweep on a single task. Note that these values were then used uniformly across all tasks.

Algorithm 1: Error Detection

Result: Success Rate S

Input: $\Phi, \psi, K, H, \pi, T, O, \rho_0, \xi_0$

Initialize $t, k, S \leftarrow 0, s \sim \rho_0, o \sim \xi_0,$

$\beta \leftarrow \emptyset$

while True do

if success then

$S \leftarrow 1;$

`terminate()`;

end

`append`(β, o);

if $t > H$ then

$\epsilon = \Phi(\beta[t-H], \beta[t]);$

if $\epsilon > \psi$ then

$k++ = 1;$

if $k == K$ then

`terminate()`;

else

$\epsilon = \text{recover}();$

if $\epsilon > \psi$ then

`terminate()`;

end

end

end

end

$a \sim \pi(o);$

$s \sim T(\cdot | s, a);$

$o \sim O(s, a);$

end

Table A.1: **Algorithm Hyperparameters:** We show selected hyperparameters used for our models during experiments. BC-TieredRNN and BC-RNN parameters were chosen such that the total parameter count was roughly the same. ReLMoGen parameters were chosen to match those presented in [45].

Algorithm	Hyperparameter	Value	
BC-TieredRNN	LR	$1e - 4$	
	Sequence Length	50	
	GMM Prior	True	
	N GMM Modes	5	
	RNN Horizons	[50, 5]	
	RNN Strides	[1, 10]	
	RNN Tier Hidden Dims	[1000, 400]	
	RNN Tier z_i Dim	32	
Actor MLP Dims	[300, 400]		
BC-RNN	LR	$1e - 4$	
	Sequence Length	50	
	GMM Prior	True	
	GMM Num Modes	5	
	RNN Horizons	50	
	RNN Tier Hidden Dims	1200	
	Actor MLP Dims	[300, 400]	
ReLMoGen	Actor LR	$1e - 4$	
	Sequence Length	50	
	GMM Prior	True	
	N GMM Modes	5	
	RNN Horizons	[50, 5]	
	RNN Strides	[1, 10]	
	RNN Tier Hidden Dims	[1000, 400]	
	RNN Tier z_i Dim	32	
	Actor MLP Dims	[300, 400]	
	Error Detector	LR	$1e - 3$
		Sequence Length	10
KL Weight		$1e - 5$	
VAE GMM Prior		True	
VAE GMM Latent Dim		16	
VAE GMM Num Modes		10	
VAE Encoder MLP Dims		[300, 400]	
VAE Decoder MLP Dims		[300, 400]	
VAE Prior MLP Dims	[128, 128]		
ψ	0.05		

A.4 MoMaRT Interface

In this section, we describe the specific details of our MOMART interface. A visual overview of our interface is shown in Fig. A.1. By default, To allow flexibility while minimizing operator overload, we leverage multi-view interface. By default, operators are presented with the manipulation view (Fig. A.1 left), allowing them to toggle grasping or reset the arm configuration by pressing the large, easy-to-tap buttons. To navigate, the user can hold down the virtual joystick, which will transform the view into navigation mode (Fig. A.1 right), allowing them to control the robot’s base. As with the original RoboTurk interface, the robot’s end-effector is controlled by simply moving the smartphone; this motion is tracked and converted into corresponding 6DOF commands for the end-effector.

By using this multi-view interface, users have the ability to navigate and control the arm at the same time without being overloading by the amount of content on the screen at a given time. Furthermore, an hourglass joystick interface was chosen instead of a full 360 degree joystick so that the mobile manipulator can also be allowed to turn in place at variable speed, enabling flexibility for the user to either slowly turn in tight corners or quickly rotate. Because our virtual joystick lacks haptic feedback, we create a dead-zone, shown in white (Fig. A.1 right), that prevents any acciden-

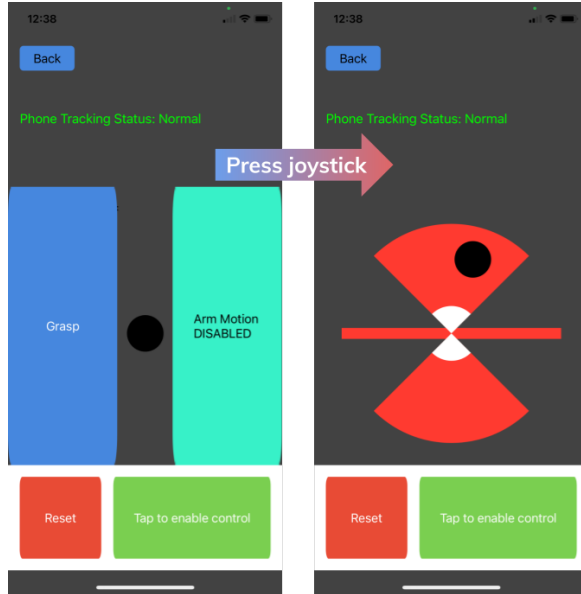


Figure A.1: MOMART interface showcasing the user interface. Users by default are presented with the manipulation view (left), allowing them to reset the arm or toggle grasping. By holding down the virtual joystick, the navigation view (right) immediately appears, allowing the user to drag the virtual joystick to navigate the robot base accordingly. The hourglass section allows for a combination of linear and rotational velocity, and the horizontal section allows for pure rotation.

Statement	Disagree (1) to Agree (5)
The interface was easy to understand and control	3.5 ± 1.1
Except for the occasional stutters, movement between the robot and my arm felt natural	3.3 ± 1.1
I felt in control of the robot as I was teleoperating	3.4 ± 1.2
By the end of the session, I felt confident in my ability to solve the task	3.3 ± 1.5
The automatic reset arm functionality was helpful to use during demonstrations	4.8 ± 0.4

Table A.2: **MOMART Study:** After 30 minutes of playtesting, new users found that the interface was comfortable to use, and marginally agreed about the system’s ease of usage and controlling the robot. Common feedback cited multiple limitations of teleoperating mobile manipulators, including limited field of view and lack of perceptual feedback for detecting collisions. However, users unanimously agreed that the ability to reset the arm to a stable configuration was helpful, validating our crucial design decision to include this functionality.

tal presses or transitions from triggering the base movement and significantly reduces the noise in navigation.

A.5 MOMART User Study

To better understand the qualitative performance of our system, we conducted a small-scale user study conducted over the course of 1 week with the goal of evaluating our platform’s efficacy. 10 users who had never used the MOMART platform before were given 30 minutes to try the system. Users were placed in a “warmup” kitchen environment to become familiarized with the controls for a minimum of 5 minutes. Once the users felt comfortable with teleoperating, the users were placed into the *Table Setup from Dishwasher* task and asked to solve the task for the remainder of the session. Like all of the 5 core kitchen tasks, this task requires leveraging the full capabilities of the MOMART system to manipulate objects and interact with large articulated furniture. Both during and after the session, users were asked to provide both qualitative and quantitative feedback on specific aspects of their experience. The summary of the quantitative results can be seen in Table A.5.

We find that generally, users find the interface easy to learn, but difficult to master. When asked “How long did it take to feel comfortable with the controls?”, 70% of users responded with 5 - 15 minutes, 10% with 15 - 30 minutes, and 20% with less than 5 minutes. Users also had generally favorable reviews of the overall usage of the system, and marginally agreed about the system’s ease of usage. This suggests that our platform can be quick to learn and easily adapted to by different users.

However, users often had issues controlling the robot. Common feedback cited multiple limitations of teleoperating mobile manipulators, including limited field of view and lack of perceptual feedback for detecting collisions. These comments reflect the difficulty of the MM domain, which inherit these challenges and require additional design decisions that may be unnecessary in SM or navigation. Crucially, nearly all users unanimously agreed that the automatic arm reset functionality included was beneficial to them during task demonstration, validating this key design decision and highlighting the benefits of being able to recover from poor arm configurations during long-horizon execution.

Interestingly, while users generally shared the same feedback, their task performance varied widely. 50% of users were unable to generate a task success within the 30-minute session, while the other 50% were able to generate an average of 3.2 successes, with a corresponding 56% average success rate. We note that most users only used about 15 minutes of their 30-minute session to try to solve the task, and those who were unable to solve the full task were still able to partially solve it. Indeed, many of these users were close to solving the full task by the end, and we would expect them to reach their first success soon if given additional playtest time. This highlights the complex nature of our tasks, which are both long-horizon and require multiple successful interactions that can require careful precision and rotation-heavy movement not often explored in other data-driven works.

While the learning curve can be more steep compared to tabletop manipulation [35], it is promising that 50% of new users with no prior experience with MOMART can immediately start generating task successes after less than 30 minutes of task interaction. As a first-of-its kind interface, we hope that future work can build upon this platform to increase its intuitiveness for people. Moreover, despite the challenges faced with this platform, the merits are clear in the ultimate scale of data

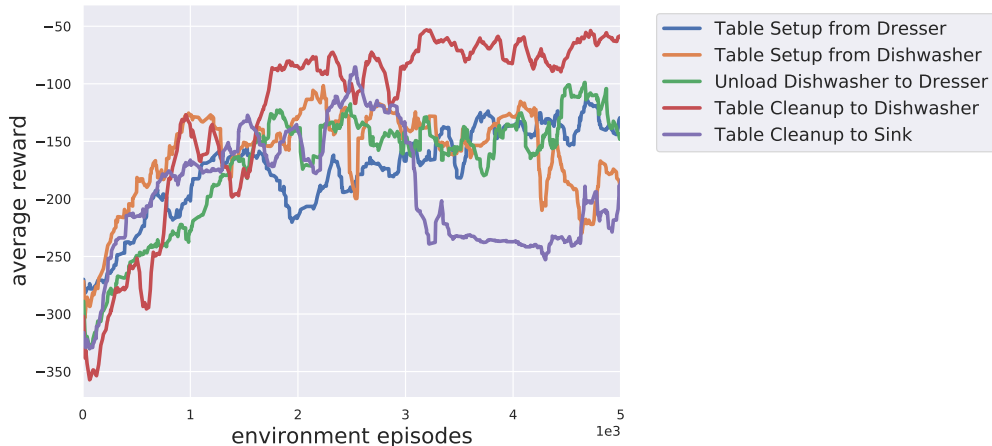


Figure A.2: Training progress for ReLMoGen. For all tasks, the agent is able to learn to get nearer the bowl but not the subsequent manipulation actions needed to complete the task.

and learning results we have been able to produce, and motivate additional research in the area of large-scale datasets for mobile manipulation.

A.6 ReLMoGen Results

We trained the SAC variant of ReLMoGen [45] baseline with a slightly modified version of the original implementation. Since the original action space of ReLMoGen would make it impossible to finish our tasks, given that they require the ability to grasp and to move the end effector in free space, our only modification was to expand the action space. Instead of only choosing between using motion planning for navigation or manipulation, and third scalar output was added to the action space that would allow the agent to use the pose and gripper control space that is used by the imitation learning agents. This makes it possible for the trained agents to accomplish the tasks, while still using the motion-planning based actions from the original model. The need to use this expanded action space is why we used the SAC variant of ReLMoGen instead of the DQN variant, since the latter outputs Q value maps instead of an action vector that is incompatible with the expanded action space.

All tasks were kept the same as they were for imitation learning, except that a reward function was added to enable RL. All tasks have a mix of shaped and sparse reward: there is a negative l2 reward based on the distance of the end effector to the bowl, since all tasks involve grasping the bowl as their initial sub-task, and each further sub-task (grasping the bowl, possibly removing trash from the bowl, and placing the bowl in an appropriate location) results in an addition of 1 per step for the rest of the episode. This reward was chosen since there is no easy way to provide a shaped reward for the subtasks of grasping the bowl, emptying it, or placing it anywhere on a piece of furniture. In all cases, the agent never got beyond the first phase of getting nearer the bowl, indicating the difficulty of learning to grasp or manipulate objects with a sparse reward.

A.7 TieredRNN Details

Here, we provide some further context justifying our choice of TieredRNN over RNN as our final evaluation model that might not be as readily apparent from our core results. We found during preliminary hyperparameter sweeping that the TieredRNN scales better than the RNN model given similar total parameter counts; that is, further increasing the RNN model’s parameter count via the hidden dimension size generally resulted in policy degradation. Moreover, we found the TieredRNN model to also provide performance gains on previous iterations of tasks that were not included in this work. These empirical observations led us to deem the TieredRNN valuable enough to include as our final evaluation model, despite providing marginal benefits in this specific setting. We hope to continue iterating on this model in future work.

Task	Metric	Reconstruction Error (ours)	KL Divergence Error	VAE Encoder Variance Mean	VAE Encoder Variance Max	Policy Log Probability
Table Cleanup to Dishwasher	Precision	96.4 ± 2.6	86.7 ± 9.4	55.6 ± 19.2	61.1 ± 20.8	85.1 ± 8.2
	Recall	100.0 ± 0.0	94.9 ± 3.6	20.6 ± 6.0	40.3 ± 15.0	84.0 ± 6.4
Table Cleanup to Sink	Precision	97.2 ± 3.9	63.2 ± 5.6	53.3 ± 5.4	46.7 ± 11.9	64.5 ± 2.6
	Recall	86.5 ± 10.3	86.7 ± 9.6	100.0 ± 0.0	100.0 ± 0.0	93.0 ± 9.9
Table Setup from Dresser	Precision	100.0 ± 0.0	88.9 ± 15.7	26.7 ± 4.7	26.7 ± 4.7	47.9 ± 23.2
	Recall	85.9 ± 10.0	45.6 ± 21.4	100.0 ± 0.0	100.0 ± 0.0	47.2 ± 12.3
Table Setup from Dishwasher	Precision	88.2 ± 10.2	93.5 ± 4.9	47.8 ± 11.3	42.2 ± 5.7	55.4 ± 3.7
	Recall	100.0 ± 0.0	92.3 ± 10.9	100.0 ± 0.0	100.0 ± 0.0	93.3 ± 6.6
Unload Dishwasher to Dresser	Precision	85.8 ± 5.3	93.9 ± 8.6	50.9 ± 6.5	43.5 ± 10.0	69.2 ± 9.5
	Recall	100.0 ± 0.0	56.1 ± 11.9	58.3 ± 12.0	26.1 ± 11.6	85.0 ± 2.2

Table A.3: **Error Detector Comparisons:** We consider multiple alternatives to error detection metrics, and evaluate them using our Expert demonstration dataset on all tasks. The best model (bolded) is determined by averaging the error detector’s precision and recall for a given task. We find that our method clearly outperforms all other alternatives, and is able to distinguish true errors with high accuracy, while other methods tend to be much more noisy and overly conservative (low precision).

Task	Train via Finetuning (ours)	Train from Scratch
Table Cleanup to Dishwasher	14.1 ± 3.2	4.8 ± 1.4
Table Cleanup to Sink	11.5 ± 6.4	7.8 ± 4.0
Table Setup from Dresser	14.4 ± 4.7	8.1 ± 2.9
Table Setup from Dishwasher	26.3 ± 1.4	15.6 ± 4.0
Unload Dishwasher to Dresser	13.3 ± 2.4	8.9 ± 2.7

Table A.4: **Few-Shot Generalization Ablation Study:** In the domain shift setting, pretraining our IL models on our original expert data and then finetuning using few-shot demonstrations shows better policy performance across all tasks compared to solely training from scratch using the few-shot demonstrations.

A.8 Error Detector Comparison

To better understand the relative performance of our error detection method, we evaluate multiple error metric alternatives. In addition to our main reconstruction loss metric, we consider another loss metric (KL Divergence loss for the VAE model), latent metrics (VAE Encoder Variance Mean / Max values), and a policy uncertainty metric (policy action log probability). For fair comparison, we quickly tune these baselines by viewing rollouts from a single seed on a single task, and heuristically choose the best threshold error value, and set $\psi_{KL} = 35.0$, $\psi_{enc.mean} = 0.0011$, $\psi_{enc.max} = 0.0017$, and $\psi_{\pi.lp} = 17.0$. Note that for the policy log probability metric, we assume low probabilities correspond to error states; moreover, because we utilize a GMM policy, the log probabilities can span multiple orders of magnitude. For these reasons, we consider the negative log of the log probability. We test these methods utilizing the same procedure as our core experiments, evaluating three seeds for each error detector trained using the expert demonstration dataset on each task, and recording the error detector precision and recall statistics from 30 rollouts for each seed. Our results can be seen in Table A.3.

We find that across all tasks, our method easily outperforms all baselines, and achieves consistently high precision and recall rates. This further validates prior work [53, 54, 55, 56] that has found reconstruction error to be a viable metric for detecting errors, and also highlights the value of our method’s ability to be easily tuned and robust across multiple tasks, which is a property not apparent in the other baselines. Indeed, we found that for the latent and log probability methods, the error signal was very noisy and did not necessarily transfer well between tasks given the same threshold ψ value.

The best baseline is the KL Divergence method, which is the only method to achieve near- or even marginally better precision over our method in certain tasks. This suggests that loss-based metrics can be a promising method for neural network-driven error detection methods, and motivates future research in this area.

A.9 Few-Shot Generalization Baseline

To better contextualize the challenges of few-shot generalization learning, we evaluate a baseline model that is trained from scratch exclusively on the few-shot demonstrations in the shifted domain setting. As in the case with our core results, we train each model for 30 epochs and record the average top three best evaluation success rates from 30 episodes aggregated over 3 seeds. The results can be seen in Table A.4.

We find that across all tasks, pretraining using the core dataset and finetuning on the few-shot demonstrations result in better policy performance compared to solely training on few-shot demonstrations from scratch. This validates the potential for direct transfer learning methods to provide tangible benefits in the MM setting, and suggests that information may be potentially shared across diverse task initializations.

A.10 Sim2real Potential

Due to the pandemic, we were unable to deploy our method on a real Fetch robot. However, we believe our method can transfer to the real world, because of the minimal assumptions we make. Both the teleoperator and agent are limited to on-board sensors, and are not provided any privileged information such as low-level object states or a global camera view: the imitation learning policy uses as input **only** RGB-D images and laser scan point clouds. The visual observations provided by the simulator, iGibson [62] are high-quality, with natural textures and materials rendered with a physics-based renderer, background and lighting probes obtained from real world. Moreover, the model used for our simulated robot closely aligns with the real Fetch robot, with identical sensor specifications, kinematics, and control schemes.

We do recognize there are some key limitations: the well-known gap between real and simulated physics dynamics, caused by approximated contact models, friction and misalignment in articulated joints, may be a source of some divergence in the real world. While more demonstration data may compensate for some of these discrepancies, it is unclear how much of an impact this can cause on downstream policy performance. We expect to be able to transfer part of the performance obtained with simulated data to real world, but if this demonstrates to be unfeasible, our immediate next step after the pandemic is to use MOMART to control a real mobile manipulator and collect real world data, as it has been done with similar smartphone-based systems for real-world stationary arms [57]. Because our system (teleoperation, imitation learning, and error detection) is not using any privileged information, we have high expectations that it will perform similarly as in simulation.